# Phonon mode behavior in strained wurtzite AlN/GaN superlattices

V. Darakchieva,* E. Valcheva, and P. P. Paskov

*Department of Physics and Measurement Technology, Linköping University, S-581 83 Linköping, Sweden*

M. Schubert

*Fakultät für Physik und Geowissenschaften, Universität Leipzig, 04103 Leipzig, Germany*

T. Paskova and B. Monemar

*Department of Physics and Measurement Technology, Linköping University, S-581 83 Linköping, Sweden*

H. Amano and I. Akasaki

*High-Tech Research and Department of Materials Science and Engineering, Meijo University, 1-501 Shiogamaguchi, Tempaku-ku, Nagoya 468-8502, Japan*

We have studied phonons in AlN/GaN superlattices with different periods but a constant well-to-barrier ratio using a combination of infrared spectroscopic ellipsometry and Raman scattering spectroscopy. The strain evolution in the superlattice structures is assessed by high-resolution x-ray diffraction and reciprocal space mapping. We have identified $E_1(TO)$, $A_1(LO)$ and $E_2$ localized, and $E_1(LO)$ and $A_1(TO)$ delocalized superlattice modes. The dependencies of their frequencies on in-plane strain are analyzed and discussed, and the strain-free frequencies of the superlattice modes are estimated. A good agreement between theory and experiment is found in the case of GaN localized modes, while large deviations between theoretically estimated and experimentally determined frequency shifts are observed for the AlN localized modes. The delocalization effect on the $A_1(TO)$ and $E_1(LO)$ phonons, as well as the free-carrier effect on the $E_1(LO)$ phonon are also discussed.

## I. INTRODUCTION

AlGaN/GaN heterostructures have recently attracted considerable attention due to their potential applications for high power transistors and ultraviolet emitters. Short period AlGaN/GaN and AlN/GaN superlattices (SLs) are very attractive for strain management, dislocation reduction, *p* contacts and also infrared intersubband detectors. Besides their potential applications, these heterostructures are also appealing from a purely physical point of view. Their fundamental properties can be largely affected and even determined by the spatial quantization of the electron states, the anisotropy of the crystal structures and the strains in the different constituents of the heterostructures. Despite the strong research interest, only a few reports are devoted to the vibrational properties of AlN/GaN SLs.[1–5] The physics of wurtzite group-III nitride SLs is still in its infancy and the open questions are far more numerous than the existing answers.

Several theoretical models have been proposed in order to investigate optical phonon modes in wurtzite low-dimensional heterostructures. Five types of phonon modes in a wurtzite quasi-two-dimensional multilayer heterostructure have been inferred in a theoretical study within the framework of the dielectric continuum model and Loudon's uniaxial crystal model: propagating modes, quasiconfined modes, interface modes, confined modes and half-space modes.[6] However, this paper is focused only on the interface optical-phonon modes and electron-interface-phonon interactions in AlN/GaN quantum wells. The existence of quasiconfined modes (QC) and interface modes (IF) in AlN/GaN SLs at frequencies different from those of any layer compris-

ing the SL is predicted by theoretical studies in the framework of the dielectric continuum model.[1] Another recent theoretical study within the framework of the rigid ion model predicts the presence of localized and delocalized phonon modes in hexagonal AlN/GaN SLs.[4] According to these results the two nonpolar $E_2$ modes and polar $E_1(TO)$ and $A_1(LO)$ phonons are localized modes with frequencies close to those in bulk GaN and AlN and intensities proportional to the respective layer thickness. The theoretical model predicts that their frequencies are independent of the SL structure (for instance, thickness of the layers) if the effect of strain is neglected. In the framework of the dielectric continuum model the polar localized modes correspond to confinement modes of one of the SL layers, and the intensity of the higher harmonics of these modes is predicted to be negligibly low.[1] According to Davydov *et al.*[4] the $A_1(TO)$ and $E_1(LO)$ modes are delocalized in the SL, showing "normal" and "anomalous" behavior. The "normal" phonon line has a high intensity that does not change with the change of the SL structure, and the phonon frequencies gradually shift from the respective ones in GaN to those in AlN, proportionally to the relative content of the different nitride compounds in the SL.[4] The "anomalous" phonon line is less intense and with a frequency predicted to be in the LO interval of frequencies of GaN and AlN for the $A_1(TO)$ mode and in the TO interval of frequencies of GaN and AlN for the $E_1(LO)$ mode, respectively. In contrast to the "normal" line position, the "anomalous" phonon frequency changes with the AlN content in an inverse manner. The delocalized modes correspond to a pair of QC modes or a pair of IF modes in the dielectric con-

TABLE I. Thicknesses, $d$, and degree of in-plane strain, $\varepsilon_{xx}$, in the two constituent layers of the AlN/GaN SLs studied.

| Sample | $d_{GaN}$ (Å) | $\varepsilon_{xx}^{GaN}$ | $d_{AlN}$ (Å) | $\varepsilon_{xx}^{AlN}$ |
|--------|---------------|--------------------------|---------------|--------------------------|
| SL A | 22.8 | $-2.2 \times 10^{-4} \pm 1.3 \times 10^{-4}$ | 7.3 | $2.43 \times 10^{-2} \pm 1.4 \times 10^{-4}$ |
| SL B | 45.4 | $-8.1 \times 10^{-4} \pm 1.3 \times 10^{-4}$ | 14.3 | $2.37 \times 10^{-2} \pm 1.4 \times 10^{-4}$ |
| SL C | 88.6 | $-26.1 \times 10^{-4} \pm 1.3 \times 10^{-4}$ | 28.6 | $2.18 \times 10^{-2} \pm 1.4 \times 10^{-4}$ |

tinuum model.[1,4] We use the above notations of the SL phonon modes from Ref. 4 throughout the paper.

The crystal dynamics of low-dimensional structures containing AlN and GaN is very complex due to the fact that the phonon dispersion curves of these two compounds overlap. Moreover, the effect of strain and polarization fields on phonon modes additionally complicates the interpretation of the vibrational spectrum of a GaN/AlN SL. In addition, the formation of the SL induces a folding of the Brillouin zone in the growth direction leading to the appearance of new phonon modes. As a consequence, an unambiguous identification and assignment of the nature (localized or delocalized) of SL modes is a complicated task. Gleize *et al.* assign $E_1$(TO), $A_1$(LO) and $E_2$ modes to GaN sublayers of a 5.1-nm-AlN/6.3-nm-GaN SL studied by Raman scattering.[2] Their assignment is based on the estimations of the frequency shifts with respect to the strain-free frequencies of the respective GaN phonons combined with additional measurements on the edge surface of a beveled sample.[2] For the same SL a QC nature of some of the SL modes was assessed by a comparison of calculated and experimental phonon angular dispersions.[3] A similar approach of comparing the frequencies of modes detected in Raman spectra with theoretical predictions is used to study phonons in a 100-period 20-nm-AlN/20-nm-GaN SL.[4] As a result the authors assigned localized modes with $E_2$, $E_1$(TO) and $A_1$(LO) symmetries and estimated the strain in the sublayers from the frequency positions. Delocalized $A_1$(TO) modes with "normal" and "anomalous" behavior were also assigned, but no delocalized $E_1$(LO) mode in AlN/GaN SLs has been identified yet; the reason is believed to be the absence of delocalization effects in long period SLs.[4]

In this work we report on the study of phonons in AlN/GaN SLs with different periods but a constant well-to-barrier ratio. We used a combination of two techniques: Infrared spectroscopic ellipsometry (IRSE) and Raman scattering spectroscopy to complement each other. IRSE allows an identification of the type of modes, localized or delocalized, and high sensitivity to the $E_1$(TO) and LO phonon parameters, while Raman scattering ensures access to $A_1$(TO) and $E_2$ (not accessible by IRSE). The phonon mode behavior with strain evolution, which is independently assessed by high-resolution x-ray diffraction (HRXRD) and reciprocal space mapping (RSM), is presented and discussed.

## II. SAMPLES, EXPERIMENTAL AND MODELING PROCEDURES

Crack-free 10-period AlN/GaN SLs were grown on undoped 2-$\mu$m-thick GaN layers deposited on (0001) sapphire substrates by metalorganic vapor phase epitaxy. The structures were grown with different well thicknesses keeping the same well-to-barrier thickness ratio as 3:1. The growth parameters and thicknesses of the buffer layer and the SL constituents were chosen in order to realize crack-free growth of high quality SL structures with a high degree of coherence. Relatively thin AlN barrier layers were grown in order to enhance also delocalization effects in the SL structure. The thicknesses of the AlN barriers and GaN wells as determined by HRXRD are listed in Table I. Details about the growth and the structural and electrical properties of the SLs can be found in Refs. 7 and 8.

The HRXRD and RSM were performed using a Philips triple axis diffractometer following the measurement procedure described in Ref. 9. A parabolic graded multilayer mirror collimator, followed by a channel-cut 2-bounce Ge(220) monochromator on the primary side and an asymmetric 2-bounce Ge(220) analyzer crystal giving a resolution of 36 arcsec (around $2\theta = 30° - 40°$) were used. Both $a$ and $c$ lattice parameters of the GaN buffer layer were measured using several symmetric and asymmetric reflections,[10,11] and the out-of-plane and in-plane strains were estimated using as strain-free lattice parameters those reported for GaN powder.[12] The $a$ lattice parameters of the AlN and GaN sublayers of the SLs were determined from the satellite peaks in the RSMs around the GaN 104 reciprocal lattice point. The lattice parameters of the two sublayers were assumed to be equal. We note that if the AlN and GaN sublayers exhibit slightly different lattice parameters this assumption will render an average value for the lattice parameter. The in-plane strain in the two SL constituents was also estimated by using as strain-free lattice parameters those of GaN and AlN powders, respectively.[12] The values of the in-plane strain in the AlN and GaN sublayers of the SLs and their standard deviations are given in Table I.

Room-temperature IRSE measurements were performed in the spectral range of 350–1500 cm$^{-1}$ with a spectral resolution of 2 cm$^{-1}$, and at 60° and 70° angles of incidence. Ellipsometry determines the ratio of the complex reflection coefficients $R_p$ and $R_s$ for light polarized parallel ($p$) and perpendicular ($s$) to the plane of incidence, respectively,[13]

$$\rho = R_p/R_s = \tan \Psi \exp(i\Delta), \qquad (1)$$

where $\Psi$ and $\Delta$ denote the ellipsometric angles. A regression analysis is necessary to obtain the IR optical properties from the IRSE data. The IRSE data were modeled using a four-phase model: ambient/SL stack/GaN buffer layer/substrate. The HRXRD study showed that the SLs consist of well-defined sublayers, which allows us to treat the SL stack in

the model as built up of alternating AlN barrier and GaN well layers with thicknesses as determined from HRXRD (Table I). A prerequisite for the data analysis is the precise knowledge of the sapphire dielectric function, which was reported by Schubert et al.,[14] and it was taken without any changes in the present work. The anisotropic AlN and GaN dielectric functions were parametrized along ($j=\parallel$) and perpendicular ($j=\perp$) to the $c$ axis, accounting for the polar phonon contribution:[13,15]

$$\epsilon_j^L(\omega) = \epsilon_{\infty,j} \frac{\omega^2 + i\gamma_{LO,j}\omega - \omega_{LO,j}^2}{\omega^2 + i\gamma_{TO,j}\omega - \omega_{TO,j}^2}, \qquad (2)$$

where $\omega_{TO,\perp}$, $\omega_{TO,\parallel}$, $\omega_{LO,\perp}$ and $\omega_{LO,\parallel}$ denote the frequencies of the $E_1(TO)$, $A_1(TO)$, $E_1(LO)$ and $A_1(LO)$ modes of the respective layer, and $\gamma_{TO,\perp}$, $\gamma_{TO,\parallel}$, $\gamma_{LO,\perp}$, $\gamma_{LO,\parallel}$ are the corresponding mode broadening parameters. $\epsilon_{\infty,\perp}$ and $\epsilon_{\infty,\parallel}$ are the high-frequency limits for polarization perpendicular and parallel to the $c$ axis. A possible contribution from free carriers to the dielectric function are also accounted for in the dielectric function of the GaN buffer and GaN SL sublayers:[13,15]

$$\epsilon^{(FC)}(\omega) = -\frac{(\omega_p^*)^2}{\omega(\omega + i\gamma_p)}, \qquad (3)$$

with

$$\omega_p^* = e\sqrt{\frac{N}{\epsilon_0 m}}. \qquad (4)$$

The unscreened plasma frequency $\omega_p^*$ depends on the free-charge-carrier concentration $N$, and effective mass $m$ and $\epsilon_0$ is the vacuum permittivity, and $e$ is the electrical unit charge. The plasmon broadening parameter $\gamma_p$ is related to the optical free-charge-carrier mobility $\mu$:[13]

$$\gamma_p = \frac{e}{m\mu}. \qquad (5)$$

The model parameters that were allowed to vary during the IRSE data analysis are the frequency and broadening parameters of the $E_1(TO)$, $E_1(LO)$ and $A_1(LO)$ modes of the buffer layer and the SL constituents, the high-frequency limit of the dielectric function, $\epsilon_\infty$, the carrier concentration and moblity, and the thickness of the buffer layer. Due to the $c$-plane orientation of the SLs, the IRSE data are not sensitive to the TO resonance frequency with the polarization vector parallel to the sample normal.[14] Consequently, the $A_1(TO)$ phonon mode resonance could not be found and the values determined from the Raman measurements were used in the calculated data as fixed parameters. The thickness values of the SL constituents as determined from HRXRD (Table I) were kept constant during the regression analysis. The nature of a particular SL mode was suggested based on the IRSE data analysis in the following way. A localized mode is such mode for which the polarazability contribution according to Eqs. (2) and (3) needed to be considered either in the GaN or in the AlN sublayers only. In contrast, a delocalized mode needed to be included into the dielectric func-
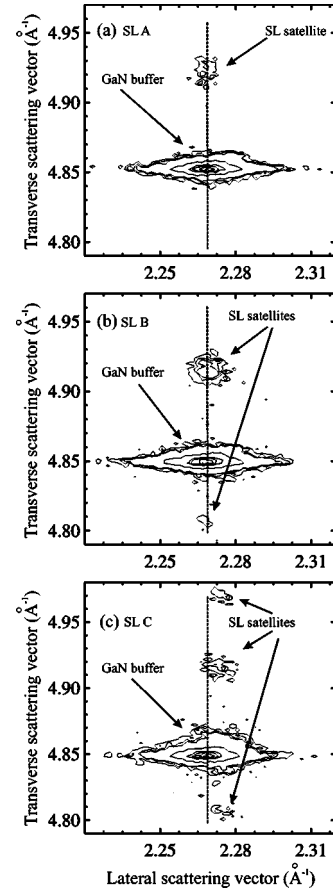


FIG. 1. RSMs around the GaN 104 reciprocal space point of the three SLs studied: (a) SL A, (b) SL B and (c) SL C. The diffraction from the GaN buffer layer and the SL satellites are indicated. The vertical dashed lines mark the position of pseudomorphic growth of the SL structures on the underlaying buffer layers.

tion models for both SL constituents simultaneously. Further details about the data analysis can be found in Ref. 13 and references therein.

Micro-Raman measurements were carried out at room temperature on a Microdil 28 Dilor triple spectrometer at 488 nm excitation. The diameter of the laser spot on the samples was 1 $\mu$m and the spectral resolution was about 1 cm$^{-1}$. The experiment was conducted in a backscattering configuration with the $z$ direction oriented along the SL $c$ axis. Two scattering geometries were used: $z(xx)\bar{z}$ allowing $E_2$ and $A_1(LO)$, and $x(zz)\bar{x}$ allowing $A_1(TO)$ modes to be detected, respectively.[16]

## III. RESULTS AND DISCUSSION

### A. Strain evolution

RSMs around the GaN 104 reciprocal space point of the three SLs studied are shown in Fig. 1. Diffraction from the reciprocal space point of the GaN buffer layer and the satellites associated with the SLs are seen. The $a$ and $c$ lattice parameters of the GaN buffer are determined to be $a = 3.1886$ Å and $c = 5.18522$ Å for all three SLs. A comparison with the strain-free lattice parameters[12] shows that the

GaN buffer layer experiences a small compressive in-plane strain $e_{xx}=-2.2\times10^{-4}$ and a small tensile out-of-plane strain $e_{zz}=2.3\times10^{-5}$. The vertical lines in Fig. 1 mark the locations where diffraction from the reciprocal lattice points of pseudomorphically grown AlN/GaN SLs on the buffer layer would appear. It is clearly seen that the short-period SL A is grown coherently on the GaN buffer layer and both the barrier and the well have the same in-plane lattice parameter as the underlying GaN buffer layer. In other words there is a large tensile in-plane strain in the AlN sublayers and a small compressive in-plane strain in the GaN wells (see Table I). The RSM of the SL B (Fig. 1) shows that the structure is not pseudomorphic to the underlying buffer layer anymore, but the disturbance of the pseudomorphic growth is still small. A distortion of the pseudomorphic growth is expected to occur with increasing the AlN barrier thickness as a result of initial strain relaxation in the AlN sublayers (see Table I). This partial strain relief in the barriers consequently leads to an increase of the compressive strain in the GaN wells. A further deviation from the pseudomorphic growth of the SL structure with increasing barrier thickness is seen in the RSM of the SL C. Hence, the AlN sublayers of SL C are more relaxed and the GaN sublayers are further strained (Table I). The presence of SL satellite peaks of high order in the RSM of SL C [Fig. 1(c)] is indicative of high crystal quality, good periodicity and low defect density, despite the strain relaxation process advancing. We note that all SLs are crack-free, which suggests that their coherence is preserved, even when the SL structure is not pseudomorphic to the underlaying GaN buffer layer.[17] The latter justifies also the used assumption of equal lattice parameters of barrier and well layers.

### B. Phonon mode identification

Figures 2(a) and 2(b) show experimental and calculated $\Psi$ and $\Delta$ spectra, respectively, for the three SLs. The IRSE spectra are highly sensitive to the frequency and broadening parameter of the $E_1(TO)$ and $A_1(LO)$ modes. Typically, distinct spectral features appear near the two resonances, but the appearance of a spectral structure related to the $A_1(LO)$ mode depends on the film thickness, layer sequence and mode broadening. The parameters of the $E_1(LO)$ modes can be determined from the line shape analysis of the IRSE data although there is no feature related to it.

As a result of the IRSE data modeling phonon modes originating from the GaN buffer layers and the SLs were identified. The frequencies and broadening parameters of the $E_1(TO)$, $A_1(LO)$ and $E_1(LO)$ modes from the GaN buffer layer were extracted with very small standard deviations of $0.1$–$0.2$ cm$^{-1}$. These modes appear at frequencies slightly higher than those determined for bulk (assumed as strain-free) GaN,[18] as expected in the case of compressive in-plane strain. We calculated an in-plane strain $e_{xx}=-4\times10^{-4}$ in the buffer layer from the observed mode shifts and using the GaN deformation potentials and stiffness constants.[16,19] Having in mind that the uncertainties of the stiffness constants and deformation potentials are relatively large the calculated value of the in-plane strain in the GaN buffer layer is in a good agreement with the RSM result of $-2.2\times10^{-4}$. The
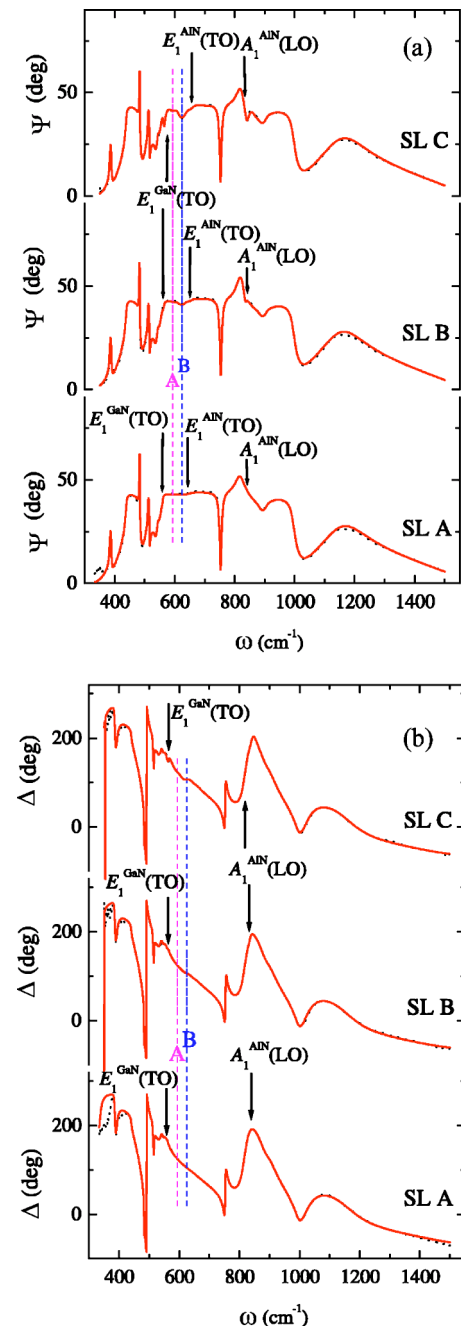


FIG. 2. Experimental (dots)and calculated (solid lines) IRSE (a) $\Psi$ and (b) $\Delta$ spectra for the three SLs studied at 70° angle of incidence. The phonon modes originating from the SL constituents are indicated. Two delocalized modes, A and B, not predicted by the theory are also indicated.

best-fit to the IRSE data gives a free-carrier concentration in the buffer layer below the IRSE detection limit ($1\times10^{17}$ cm$^{-3}$ for *n*-type GaN).[15]

In addition, we have identified from the IRSE the following phonon modes originating from the SLs: (i) localized $E_1(TO)$ and $A_1(LO)$ in both the AlN and GaN sublayers, (ii) delocalized $E_1(LO)$ phonon and (iii) delocalized modes with $E_1(TO)$ symmetry at 593 and 625 cm$^{-1}$. The first two groups of phonon modes are expected to occur according to the
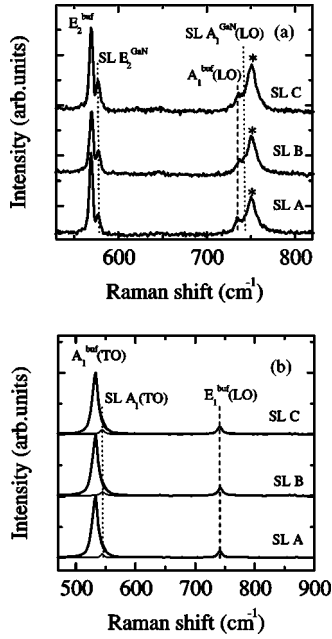
FIG. 3. Polarized Raman spectra of the three SL studied in two different backscattering configurations: (a) $z(xx)\bar{z}$ and (b) $x(zz)\bar{x}$. The phonon modes originating from the GaN buffer layer and the SL are indicated. The sapphire $E_g(s)$ mode is indicated by an asterisk in Fig. 3(a).

theoretical predictions, while the delocalized modes from the third group have not been predicted.[4] The SL phonon modes that can be related to resonance structures in the $\Psi$ and $\Delta$ are indicated in Figs. 2(a) and 2(b). The parameters of the $A_1(LO)$ originating from the GaN sublayers were determined from the IRSE data analysis with large uncertainties.

In order to obtain more accurate data for the parameters of the $A_1(LO)$ mode originating from the GaN sublayers and to study the phonons not accessible by IRSE [$E_2$ and $A_1(TO)$] we performed Raman scattering measurements. The Raman spectra of the three SLs are shown in Figs. 3(a) and 3(b), where the phonon modes originating from the GaN buffer layer and the SLs are indicated. The allowed $E_2$ and $A_1(LO)$ from the buffer layer are detected at frequencies higher than the respective strain-free values[18] in accordance with the small compressive in-plane strain in the buffer inferred by RSM and IRSE analyzes. In addition, $E_2$ and $A_1(LO)$ modes at frequencies higher than (but close to) those of the respec-

tive modes from the buffer are also identified [Fig. 3(a)] and suggested to originate from the GaN sublayers of the SLs. The frequency errors of these modes are determined from the fits to the Raman spectra to be 0.5 cm$^{-1}$ for the $E_2$ modes and between 1.4 and 2.3 cm$^{-1}$ for the $A_1(LO)$ modes, respectively. The $E_2$ and $A_1(LO)$ modes from the AlN sublayers are not detected in the Raman spectra, most probably due to the smaller barrier thickness (Table I) and poorer scattering efficiency compared to GaN. The Raman spectrum of $A_1(TO)$ symmetry [Fig. 3(b)] shows one intense line at frequency close to that of the GaN $A_1(TO)$ mode. This line is apparently asymmetric and a deconvolution with Lorentzian shape peaks suggests that it is composed by two lines: (i) $A_1(TO)$ mode from the GaN buffer layer and (ii) $A_1(TO)$ originating from the SLs, as indicated in Fig. 3(b). The SL $A_1(TO)$ frequency was extracted from the fits to the Raman spectra with an error of 0.5 cm$^{-1}$. The $E_1(LO)$ from the GaN buffer layer that is symmetry forbidden but might be activated by Fröhlich interaction or resulting from admixture of a small $A_1$ component,[20] is also observed.

### C. SL phonon modes and strain

In general, the values of the phonon frequencies in a SL are expected to depend mainly on the relative content of the different nitride in the SL and the strain. For our SLs only the strain effect is relevant, since the well-to-barrier ratio is kept constant when the SL period is changed. We analyzed the dependencies of the frequencies of all SL modes identified by IRSE and Raman on the experimentally determined by RSM in-plain strain in the respective sublayer for the localized modes and on the average in-plane strain in the case of delocalized modes. This allows us to determine the strain-free values of the SL modes and therefore to estimate the respective frequency shifts. We estimated also the errors of the frequency shifts assuming the errors of the strain-free frequencies as independent from the measurement errors. This leads to an overestimation of the errors of the frequency shifts given in Figs. 4–6.

#### 1. Localized modes

In the case of localized modes within the SL constituents, the frequency shifts are expected to depend linearly on the strain in the respective sublayer. Figures 4(a)–4(c) and Figs. 5(a) and 5(b) present the shifts of the identified localized
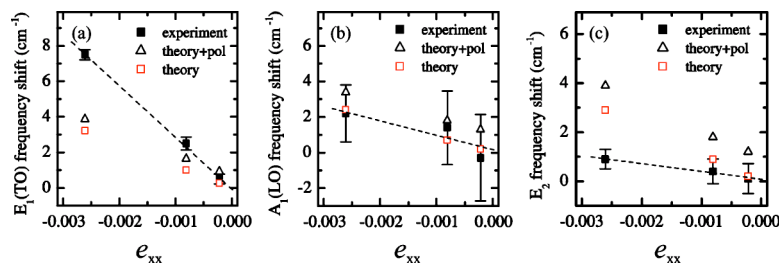


FIG. 4. Frequency shifts of the localized phonon modes in the GaN sublayers of the SLs versus the in-plain strain, $\varepsilon_{xx}$: (a) $E_1(TO)$, (b) $A_1(LO)$ and (c) $E_2$. The experimental shifts are indicated by full squares and the fits to the experimental points are given by dashed lines. The theoretical estimations for the respective frequency shifts are given with hollow squares when no polarization fields effect is considered and with hollow triangles when the latter effect is accounted for.
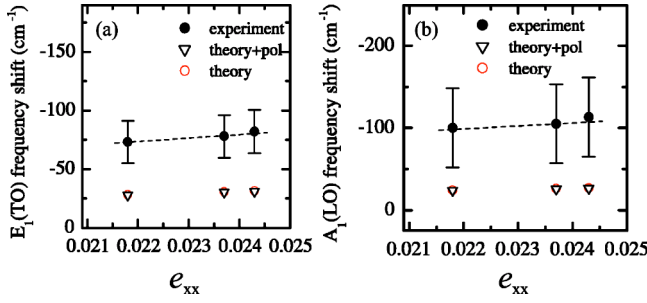
FIG. 5. Frequency shifts of the localized phonon modes in the AlN sublayers of the SLs versus the in-plain strain, $\varepsilon_{xx}$: (a) $E_1$(TO) and (b) $A_1$(LO). The experimental shifts are indicated by full circles and the fits to the experimental points are given by dashed lines. The theoretical estimations for the respective frequency shifts are given with hollow circles when no polarization field effect is considered and with hollow inverted triangles when the latter effect is accounted for.

modes versus the in-plane strain in the GaN and AlN sublayers, respectively. In addition to the experimental data theoretical estimations for the frequency shifts without and accounting for the polarization fields are also presented in Figs. 4 and 5 for comparison. The following relations are used for the theoretical estimations:

$$\Delta\omega_i^{(j)} = 2a_i^{(j)}\varepsilon_{xx} + b_i^{(j)}\varepsilon_{zz}, \tag{6}$$

and

$$\varepsilon_{zz} = -\frac{2C_{13}^{(j)}}{C_{33}^{(j)}}\varepsilon_{xx}, \tag{7}$$

when only the elasticity relationship between in-plane and out-of-plane strain are considered, and

$$\varepsilon_{zz}^{(j)} = -\frac{2C_{13}^{(j)}}{C_{33}^{(j)}}\varepsilon_{xx}^{(j)} - (-1)^j\frac{e_{33}^{(j)}}{d_jC_{33}^{(j)}\Delta}(P_{sp}^{(2)} - P_{sp}^{(1)} - 2\Delta_1\varepsilon_{xx}^{(1)} + 2\Delta_2\varepsilon_{xx}^{(2)}), \tag{8}$$

$$\Delta = \sum_{j=1}^{2}\frac{1}{d_j}\left(\epsilon_0\epsilon_{\infty,zz}^{(j)} + \frac{e_{33}^{(j)2}}{C_{33}^{(j)}}\right), \tag{9}$$

$$\Delta_j = e_{31}^{(j)} - e_{33}^{(j)}\frac{C_{13}^{(j)}}{C_{33}^{(j)}}, \tag{10}$$

when the piezoelectric and pyroelectric effects are accounted for.[21] In Eqs. (6)–(10) $a_i^{(j)}$ and $b_i^{(j)}$ are the deformation potentials of the respective mode $i$, the $C_{kl}^{(j)}$ are the stiffness constants, $e_{kl}^{(j)}$ are the piezoelectric constants, $d_j$ is the thickness, $P_{sp}^{(j)}$ is the spontaneous polarization, $\epsilon_0$ is the vacuum permittivity, and $\epsilon_{\infty,zz}^{(j)}$ is the high-frequency limit of the dielectric function of the respective SL sublayer: $j=1$ for GaN and $j=2$ for AlN. In all calculations of the frequency shifts the stiffness constants of GaN from Ref. 19 and of AlN from Ref. 22, as well as the deformation potentials of AlN from Ref. 23 were used. The deformation potentials of the GaN $E_1$(TO) mode reported in Ref. 16 were used, while for the



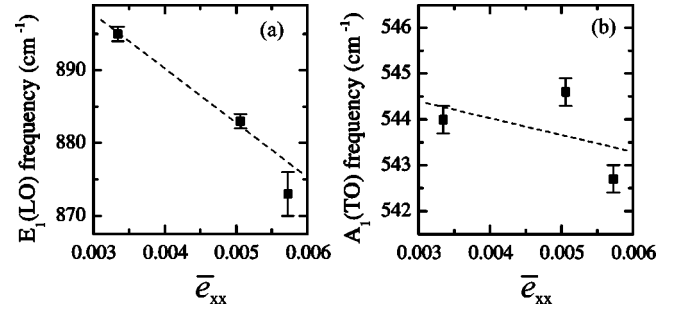FIG. 6. Frequencies of the delocalized phonon modes versus average in-plane strain in the SLs, $\bar{\varepsilon}_{xx}$: (a) $E_1$(LO) and (b) $A_1$(TO). The fits to the experimental points are given by dashed lines.

GaN $E_2$ and $A_1$(LO) phonon deformation potentials the results reported in a recent publication by Demangeot *et al.*[24] were used. The values of the spontaneous polarizations, piezoelectric constants and high-frequency limits of the dielectric functions were taken from Refs. 25 and 26.

It is seen from Figs. 4(a)–4(c) that all localized modes within the GaN sublayers of the SLs show good agreement with the theoretically estimated shifts by Eqs. (6)–(10). There is a very good agreement between theory and experiment for the $A_1$(LO) modes. The experimental $E_1$(TO) shifts appear slightly larger, while those in the case of the $E_2$ modes are slightly smaller than the theoretically estimated values. The effect of the polarization fields amounts to $0.6-1$ cm$^{-1}$, depending on the particular mode and sublayer thickness, most often being within the errors of the experimentally determined shifts. The latter is in agreement with previous theoretical findings for infinite AlN/GaN SLs with equal barrier and well thicknesses.[21] We note that although leading to subtle effect the polarization fields need to be accounted for since in real structures the change of strain is often accompanied by a change of the thickness, which inevitably leads to a change of the slope of the dependence of the mode frequency on the strain. We have determined the following strain-free frequencies for the GaN localized modes: $559.5\pm0.2$ cm$^{-1}$ for the $E_1$(TO), $741.5\pm0.8$ cm$^{-1}$ for the $A_1$(LO) and $576.9\pm0.1$ cm$^{-1}$ for the $E_2$. All these values appear slightly blueshifted with respect to the strain-free frequencies of the respective modes in bulk GaN[18] ($558.2$ cm$^{-1}$, $736.5$ cm$^{-1}$ and $567.0$ cm$^{-1}$, respectively). We note that in the case of AlAs/GaAs cubic SLs the confined modes are typically redshifted, as it was also suggested by theoretical calculations for wurtzite AlN/GaN SLs with a period of 10 nm.[1] The observed blueshift of the phonons localized in the GaN sublayers for our SLs might be due to interface disorder which was shown to have significant effect in the case of short-period SLs and has been experimentally observed for AlAs/GaAs SLs.[27] Possible delocalization effects might also be responsible for the observed blueshift of the GaN SL confined modes. Further experimental and detailed theoretical studies on SLs with different periods are needed in order to clarify this issue.

In contrast to the GaN localized modes, the strain-free frequencies of the phonons localized in the AlN sublayers appear much higher than the strain-free values of the respective modes reported for bulk AlN (Ref. 28): $727.6\pm18$ cm$^{-1}$

for the $E_1$(TO) and $941 \pm 48$ cm$^{-1}$ for the $A_1$(LO), compared to 669 cm$^{-1}$ and 890 cm$^{-1}$ for bulk AlN (Ref. 28), respectively. Accordingly, the AlN localized modes show very large shifts compared to the estimations using the elasticity theory and accounting for the polarization effects [Figs. 5(a) and 5(b)]. The observed large deviations between theory and experiment stem mostly from the large values of the standard errors for the experimentally determined strain-free frequencies. The later are mainly due to the fact that the range of in-plain strain studied is very narrow and lies far away from the zero strain. In addition, several other effects might also contribute to the large shift deviations. First of all, these are the uncertainties in the phonon deformation potentials of AlN (Ref. 29–31) that may result in an underestimation of the theoretical shifts. We estimated the frequency shifts with different values of the deformation potentials[23,29,30] and found that the obtained differences are of the order of 10–15 cm$^{-1}$. We note, however, that this effect alone can hardly account for the observed deviations between experiment and theory [Figs. 5(a) and 5(b)]. Another reason for these deviations might be a local distortion of the coherence of the SL structure in the case of SL C. Such effect is expected to be subtle but still may play a role due to the very small strain variation with increasing AlN thickness. Defects associated with strain relaxation and predominantly located in the AlN sublayers have been observed for the long-period SL C.[32] We note that they typically lead to mode broadening and may also affect the accuracy of phonon position determination. The mode frequency is determined as an average characteristic of the SL constituents, while strain-induced defects might be nonhomogeneously distributed along the AlN sublayers.

### 2. Delocalized modes

The $E_1$(LO) and $A_1$(TO) phonons, likely to be delocalized, are expected to reflect averaged SL characteristics, for instance, the average strain. For our SLs the tensile strain in the AlN barrier layers is much larger than the respective compressive strain in the GaN wells (see Table I) and will dominate the average strain value determining its sign. To illustrate the behavior of the delocalized modes their frequencies are plotted versus the average in-plane strain in the SLs in Figs. 6(a) and 6(b). The average in-plane strain was estimated via

$$\bar{\varepsilon}_{xx} = \frac{\varepsilon_{xx}^{GaN} d^{GaN} + \varepsilon_{xx}^{AlN} d^{AlN}}{d^{GaN} + d^{AlN}}. \quad (11)$$

The $E_1$(LO) mode is suggested to have delocalized nature based on the IRSE data analysis, since a better fit to the experimental points (Fig. 2) can be obtained if the $E_1$(LO) phonon contribution is accounted for in the model dielectric functions of both AlN and GaN sublayers. The $E_1$(LO) frequency shows a blueshift with decreasing the averaged tensile in-plane strain in the SLs [Fig. 6(a)]. The linear fit to the experimental frequencies gives a strain-free value of $925.2 \pm 8.4$ cm$^{-1}$ close to the AlN $E_1$(LO) frequency of 911 cm$^{-1}$ (Ref. 28). The frequency of the "normal" $E_1$(LO) line is expected to be around 796 cm$^{-1}$, much closer to the

strain-free $E_1$(LO) frequency of bulk GaN of 742 cm$^{-1}$ (Ref. 18) if a linear dependence on the relative AlN content is assumed. Therefore, reduced delocalization leading to predominant localization in the AlN sublayers may be invoked in order to explain the blueshift of the strain-free frequency of the SL $E_1$(LO) mode with respect to the estimated one for a perfectly delocalized mode. A lack of delocalization effect on the $E_1$(LO) phonon have been reported for long period AlN/GaN SLs related to the large difference in the mode frequencies of AlN and GaN (169 cm$^{-1}$) (Ref. 4). In the latter case, however, two distinct phonon lines were observed close to the frequencies of the $E_1$(LO) mode in AlN and GaN, respectively. No phonon close to the GaN $E_1$(LO) frequency could be detected by IRSE, but more investigations are needed in order to clarify this issue. We also note that the period of the AlN/GaN SLs studied in Ref. 4 is 40 nm, being much larger than the periods of our SLs which are in the range of 3–11.7 nm. The latter suggests that other effects than reduced delocalization may be involved. For instance, in the case of delocalization the LO phonons can feel in a complex manner possible free carriers filling the GaN wells. In relation to this it is worth mentioning that we obtained from the IRSE data modeling that the SL GaN sublayers contain free carriers. We assume that the carriers within the GaN sublayer system are free electrons and that all GaN well layers have the same carrier concentration. We note that due to the different polarization fields in AlN and GaN typically a two-dimensional electron gas (2DEG) is formed at the interface of undoped AlN/GaN heterostructures.[33] A presence of 2DEG with a sheet carrier concentration of the order of $10^{12}$–$10^{13}$ cm$^{-2}$ has been reported for AlN/GaN SLs (Ref. 7) and can result in electron filling of the GaN wells when the Fermi level is pinned at the surface. Free electrons in GaN SL sublayers have been previously also observed by IRSE and it was suggested that they may originate from interface and defect induced donor states.[5] The best-fit to the IRSE data for our SLs gave a carrier concentration in the GaN wells of the order of or higher than $10^{18}$ cm$^{-3}$ (corresponding to sheet carrier concentration of the order of $10^{12}$–$10^{13}$ cm$^{-2}$). At such concentrations the plasma modes will couple to the LO lattice modes and will form the so-called coupled LO-plasmon-phonon modes. This results in a shift of the zeros of the GaN sublayer dielectric function to higher frequencies. As a consequence, the delocalized SL $E_1$(LO) phonon may appear at higher frequencies compared to the noncoupled delocalized mode. In principle, the presence of free carriers should also affect the frequency of the LO phonon with polarization parallel to the $c$ axis. We note, however, that no significant free-carrier effect on the GaN localized $A_1$(LO) phonon detected in the Raman spectra can be inferred.

The SL $A_1$(TO) frequency deduced from the Raman measurement is in the strain-free frequency range of the $A_1$(TO) mode of GaN (Ref. 18) and AlN (Ref. 28), as one can expect for a delocalized $A_1$(TO) phonon with "normal" behavior. We estimated that this mode would appear at 556 cm$^{-1}$ if a linear dependence on the AlN content is assumed. This value compares well with the strain-free frequency of $545.5 \pm 3.4$ cm$^{-1}$ determined from the linear fit to the experi-
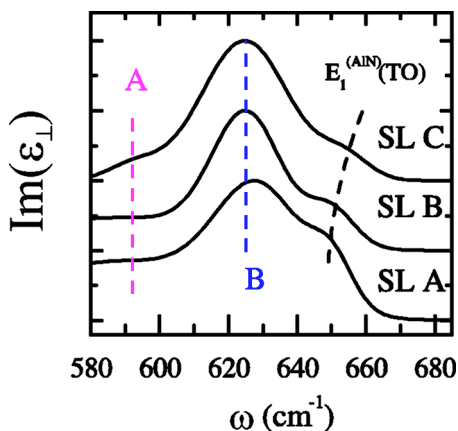
FIG. 7. Imaginary part of the AlN dielectric function perpendicular of the $c$ axis obtained from the best-fit IRSE data analysis. The AlN $E_1$(TO) localized mode and the two delocalized modes A and B are indicated.

mental $A_1$(TO) frequencies versus the averaged in-plane strain [Fig. 6(b)]. This result implies that involvement of a reduced delocalization effect on the delocalized mode behavior is not very probable in the case of the SL $A_1$(TO) mode. The latter could be understood in terms of the much smaller difference in the frequencies of the $A_1$(TO) phonon in AlN and GaN (78 cm$^{-1}$) compared to the $E_1$(LO) mode. In addition, the $A_1$(TO) phonon is not sensitive to free carriers compared to the case of LO phonons.

We have estimated that "anomalous" delocalized modes, predicted to be less intense, would appear around 841 cm$^{-1}$ and 633.5 cm$^{-1}$ for the $A_1$(TO) and $E_1$(LO) modes, respectively. No such modes could be detected by IRSE and Raman measurements [see Figs. 2 and 3(b)].

Finally, we have detected two delocalized modes with $E_1$(TO) symmetry that are not predicted by the model presented in Ref. 4. The $E_1$(TO) modes appear in the imaginary part of the dielectric function perpendicular to the $c$ axis shown in Fig. 7 for the AlN sublayers of the three SLs. The delocalized modes labeled as A and B appear at 593 and

620 cm$^{-1}$, respectively, close to the AlN $E_1$(TO) localized mode. Both features are well pronounced only in the SLs with large period and it is difficult to infer how they evolve with strain. Similar features have been observed by Raman and IRSE in AlN/GaN SLs and have been suggested to be interface excitations.[2,5] Our findings require further experimental investigations combined with theoretical modeling to be able to assess the behavior of these modes with strain evolution and to explain their origin.

## IV. CONCLUSIONS

In conclusion, we have studied the phonon behavior in AlN/GaN SLs with different periods but constant well-to-barrier ratio by combining the advantages of IRSE and Raman spectroscopy. As a result phonon modes originating from the GaN buffer layers and the SLs were detected. The following groups of SL modes were identified: (i) $E_1$(TO), $A_1$(LO) localized in both GaN and AlN sublayers of the SLs and $E_2$ mode localized in the GaN; (ii) delocalized $E_1$(LO) and $A_1$(TO) modes with "normal" behavior and (iii) delocalized modes with $E_1$(TO) symmetry around 593 and 625 cm$^{-1}$. In contrast to the first two groups, the phonons from the third group are not predicted by the theoretical model described in Ref. 4. The dependence of the SL mode frequencies on the strain were analyzed and compared with theoretical estimations within the framework of the elasticity theory and accounting for polarization effects. The strain-free frequencies of the SL modes were also estimated. Good agreement between theoretically estimated and experimentally determined frequency shifts was found in the case of the phonons localized in the GaN sublayers. In contrast, large deviations of the theoretically estimated and experimentally obtained frequency shifts were found for the AlN localized modes and possible explanations are suggested. The analysis of the delocalized mode behavior versus the average strain in the SLs allows us to draw the conclusion that reduced delocalization may play an important role in the case of the $E_1$(LO) phonon even for short-period SLs.

*Corresponding author: Electronic address: vanya@ifm.liu.se; fax: +46 13 142337; phone: +46 13 282629.

[1] J. Gleize, M. A. Renucci, J. Frandon, and F. Demangeot, Phys. Rev. B **60**, 15 985 (1999).

[2] J. Gleize, F. Damangeot, J. Frandon, M. A. Renucci, F. Widmann, and B. Daudin, Appl. Phys. Lett. **74**, 703 (1999).

[3] J. Gleize, J. Frandon, F. Damangeot, M. A. Renucci, M. Kuball, J. M. Hayes, F. Widmann, and B. Daudin, Mater. Sci. Eng., B **82**, 27 (2001).

[4] V. Yu. Davydov, A. N. Smirnov, M. B. Smirnov, S. V. Karpov, I. N. Goncharuk, R. N. Kyutt, M. V. Baidakova, A. V. Sakharov, E. E. Zavarin, W. V. Lundin, H. Harima, and K. Kisoda, Phys. Status Solidi C **0**, 2035 (2003).

[5] M. Schubert, A. Kasic, T. E. Tiwald, J. A. Woollam, V. Harle, J. Off, and F. Scholz, MRS Internet J. Nitride Semicond. Res. **5**,

W.11.39 (2000).

[6] J. J. Shi, Phys. Rev. B **68**, 165335 (2003).

[7] S. Yamaguchi, M. Kosaki, Y. Watanabe, Y. Yukawa, S. Nitta, H. Amano, and I. Akasaki, Appl. Phys. Lett. **79**, 3062 (2001).

[8] S. Yamaguchi, Y. Iwamura, Y. Watanabe, M. Kosaki, Y. Yukawa, S. Nitta, S. Kamiyama, H. Amano, and I. Akasaki, Appl. Phys. Lett. **80**, 802 (2002).

[9] V. Darakchieva, J. Birch, M. Schubert, T. Paskova, S. Tungasmita, G. Wagner, A. Kasic, and B. Monemar, Phys. Rev. B **70**, 045411 (2004).

[10] V. Darakchieva, P. P. Paskov, T. Paskova, E. Valcheva, B. Monemar, and M. Heuken, Appl. Phys. Lett. **82**, 703 (2003).

[11] V. Darakchieva, T. Paskova, P. P. Paskov, B. Monemar, N. Ashkenov, and M. Schubert, J. Appl. Phys. **97**, 013517 (2005).

[12] H. Angerer, D. Brunner, F. Freudenberg, O. Ambacher, M. Stuz-

mann, R. Höpler, T. Metzger, E. Born, G. Dollinger, A. Bergmaier, S. Karsch, and H.-J. Körner, Appl. Phys. Lett. **71**, 1504 (1997).

[13] M. Schubert, *Infrared Ellipsometry on Semiconductor Layer Structures: Phonons, Plasmons and Polaritons*, Springer Tracts in Modern Physic (Springer, Heidelberg, 2004) Vol. 209 ISBN 3-540-23249-4.

[14] M. Schubert, T. E. Tiwald, and C. M. Herzinger, Phys. Rev. B **61**, 8187 (2000).

[15] A. Kasic, M. Schubert, S. Einfeldt, D. Hommel, and T. E. Tiwald, Phys. Rev. B **62**, 7365 (2000).

[16] V. Yu. Davydov, N. S. Averkiev, I. N. Goncharuk, D. K. Nelson, I. P. Nikitina, A. S. Polkovnikov, A. N. Smirnov, M. A. Jacobson, and O. K. Semchinova, J. Appl. Phys. **82**, 5097 (1997).

[17] S. Einfeldt, H. Heinke, V. Kirchner, and D. Hommel, J. Appl. Phys. **89**, 2160 (2001).

[18] A. R. Goñi, H. Siegle, K. Syassen, C. Thomsen, and J. M. Wagner, Phys. Rev. B **64**, 035205 (2001).

[19] M. Yamaguchi, T. Yagi, T. Azuhata, T. Sota, K. Suzuki, S. Chichibu, and S. Nakamura, J. Phys.: Condens. Matter **9**, 241 (1997).

[20] F. Demangeot, J. Groenen, J. Frandon, M. A. Renucci, O. Briot, S. Clur, and R. L. Aulombard, Appl. Phys. Lett. **72**, 2674 (1998).

[21] J. Gleize, J. Frandon, M. A. Renucci, and F. Bechstedt, Phys. Rev. B **63**, 073308 (2001).

[22] L. E. McNeil, M. Grimsditch, and R. H. French, J. Am. Ceram. Soc. **76**, 1132 (1993).

[23] J. M. Wagner and F. Bechstedt, Appl. Phys. Lett. **77**, 346 (2000).

[24] F. Demangeot, J. Frandon, P. Baules, F. Natali, F. Semond, and J. Massies, Phys. Rev. B **69**, 155215 (2004).

[25] F. Bernardini, V. Fiorentini, and D. Vanderbilt, Phys. Rev. B **56**, R10 024 (1997).

[26] F. Bernardini, V. Fiorentini, and D. Vanderbilt, Phys. Rev. Lett. **79**, 3958 (1997).

[27] J. Spitzer, I. Gregora, T. Ruf, M. Cardona, K. Ploog, F. Briones, and M. I. Alonso, Solid State Commun. **84**, 275 (1992).

[28] M. Kuball, J. M. Hayes, A. D. Prins, N. W. A. van Uden, D. J. Dunstan, Y. Shi, and J. H. Edgar, Appl. Phys. Lett. **78**, 724 (2001).

[29] V. Darakchieva, P. P. Paskov, T. Paskova, J. Birch, S. Tungasmita, and B. Monemar, Appl. Phys. Lett. **80**, 2302 (2002).

[30] J. Gleize, M. A. Renucci, J. Frandon, E. Ballet-Amalric, and B. Daudin, J. Appl. Phys. **93**, 2065 (2003).

[31] J.-M. Wagner and F. Bechstedt, Phys. Rev. B **66**, 115202 (2002).

[32] E. Valcheva, T. Paskova, G. Z. Radnoczi, L. Hultman, B. Monemar, H. Amano, and I. Akasaki, Physica B **340–342**, 1129 (2003).

[33] O. Ambacher, B. Foutz, J. Smart, J. R. Shealy, N. G. Weimann, K. Chu, M. Murphy, A. J. Sierakowski, W. J. Schaff, L. F. Eastman, R. Dimitrov, A. Mitchell, and M. Shtuzmann, J. Appl. Phys. **87**, 334 (2000).